Environ. Sci. Technol. **2006**, *40,* 5304−5311

High-Resolution Depositional Records of Polycyclic Aromatic Hydrocarbons in the Central Continental Shelf Mud of the East China Sea

ZHIGANG GUO,*,† TIAN LIN,† GAN ZHANG,‡ ZUOSHENG YANG,† AND MING FANG§

College of Marine Geosciences, Ocean University of China, Qingdao 266003, China, State Key Laboratory of Organic Geochemistry, Guangzhou Institute of Geochemistry, Chinese Academy of Sciences, Guangzhou 510640, China, and Institute for The Environment, The Hong Kong University of Science and Technology, Clearwater Bay, Hong Kong, China

A well-placed ^{210}Pb-dated sediment core extracted from the distal mud in the central continental shelf of the East China Sea is used to reconstruct the high-resolution atmospheric depositional record of polycyclic aromatic hydrocarbons (PAHs), believed to be transported mainly from China in the past 200 years due to the East Asian Monsoon. Total PAHs (TPAHs), based on the 16 USEPA priority PAHs, range from 27 in 1788 to 132 ng g^{-1} in 2001. TPAH variation in the core reflects energy usage changes and follows closely the historical economic development in China. PAHs in the core are dominantly pyrogenic in source, i.e., they are mainly from the incomplete combustion of coal and biomass burning. Several individual PAHs suggest that contribution from incomplete petroleum combustion has increased during recent years. Analysis of the 2 + 3 ring and the 5 + 6 ring PAHs and principle component analysis provide more evidence in the change in the energy structure, especially after 1978 when China embarked on the "Reform and Open" Policy, indicating the transformation from an agricultural to an industrial economy of China. The historical profile of PAH distribution in the study area is obviously different from the United States and Europe due to their difference in energy structure and economic development stages.

Introduction

Polycyclic aromatic hydrocarbons (PAHs), known carcinogens and mutagens, are mainly attributed to combustion processes including the burning of fossil fuels, municipal wastes, and biomass (*1*−*5*). Other sources include crude oil seepage and diagenesis of organic matter in anoxic sediments (*6*, *7*). Airborne PAHs can enter an aquatic environment via atmospheric transport. PAHs in sediments are effective proxies for the revelation and reconstruction of industrialization and urbanization (*8*−*13*) because PAHs are mostly anthropogenic in origin. It has been reported that PAH concentrations and depositional fluxes increased in sediment cores since the Industrial Revolution due to the widespread use of fossil fuels (*4*, *8*−*10*, *12*, *13*).

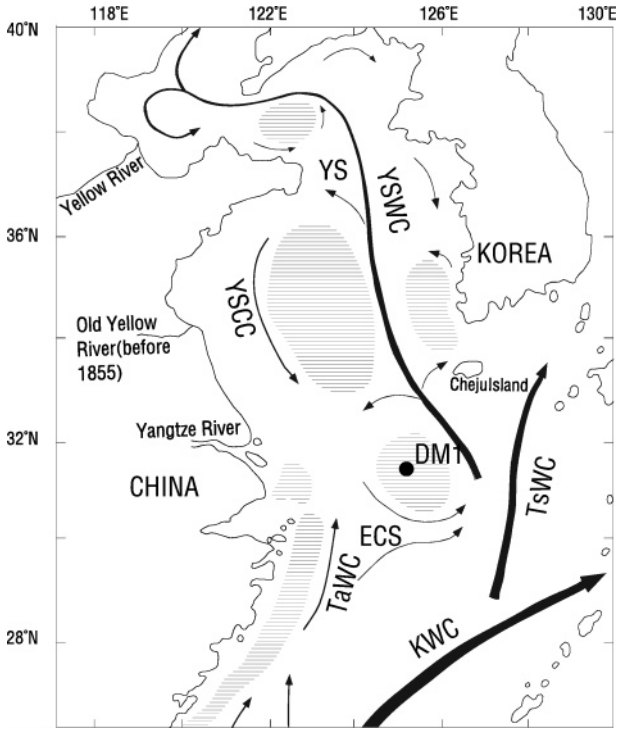

FIGURE 1. Study area, general circulation system in the Yellow Sea and East China Sea, and location of sampling site. Circulation system and mud areas (dark areas) are after ref *14*. ECS: East China Sea; YS: Yellow Sea; KWC: Keroshio Warm Current; TaWC: Taiwan Warm Current; TsWC: Tsushima Warm Current; YSCC: Yellow Sea Coastal Current; YSWC: Yellow Sea Warm Current.

The rapid economic development in China in the past three decades has, unfortunately, also polluted the environment. Historical pollution data would be very useful in understanding the impact of economic development on the environment. One way is to reconstruct such data from sediment core samples in a lake, estuary, or continental shelf.

There are several distributed mud patches in the midst of the coarser ambient silt and sand sediments on the Yellow Sea (YS) and East China Sea (ECS) (Figure 1). Distal mud (DM) is located in the central shelf of the ECS southwest to Cheju Island, Korea. DM is a modern depositional center in the ECS (*15*, *16*) and is ∼400 km from the major pollution source—the Chinese Mainland. Sediments in this region are mainly from the resuspension by tidal current and storms in winter and spring in the Old Huanghe (Yellow River) Estuary in northern Jiangsu Province (*17*) and are transported to the DM by the Yellow Sea Coastal Current (YSCC) (*16*, *17*). The Huanghe changed course to its current Bohai Sea estuary in 1855 before China started to industrialize. Thus, the sediments from the Old Huanghe Estuary to DM contain only minor anthropogenic material (*18*). Sediment contribution from the Changjiang (Yangtze River) to DM is very small because it is obstructed by the strong Taiwan Warm Current (TaWC) (*17*). During the winter and spring East Asian Monsoon when the northwesterly winds prevail, the aerosol loading in North China is very high (*19*, *20*). Driven by the East Asian monsoon, East Asian pollutants can be transported to the northern Pacific Ocean (*21*). Therefore, the ECS is

* Corresponding author phone: (86) 532 82032460; fax: (86) 532 82032799; e-mail: guozgg@ouc.edu.cn.
† Ocean University of China.
‡ Chinese Academy of Sciences.
§ The Hong Kong University of Science and Technology.

10.1021/es060878b CCC: $33.50

Published on Web 08/08/2006

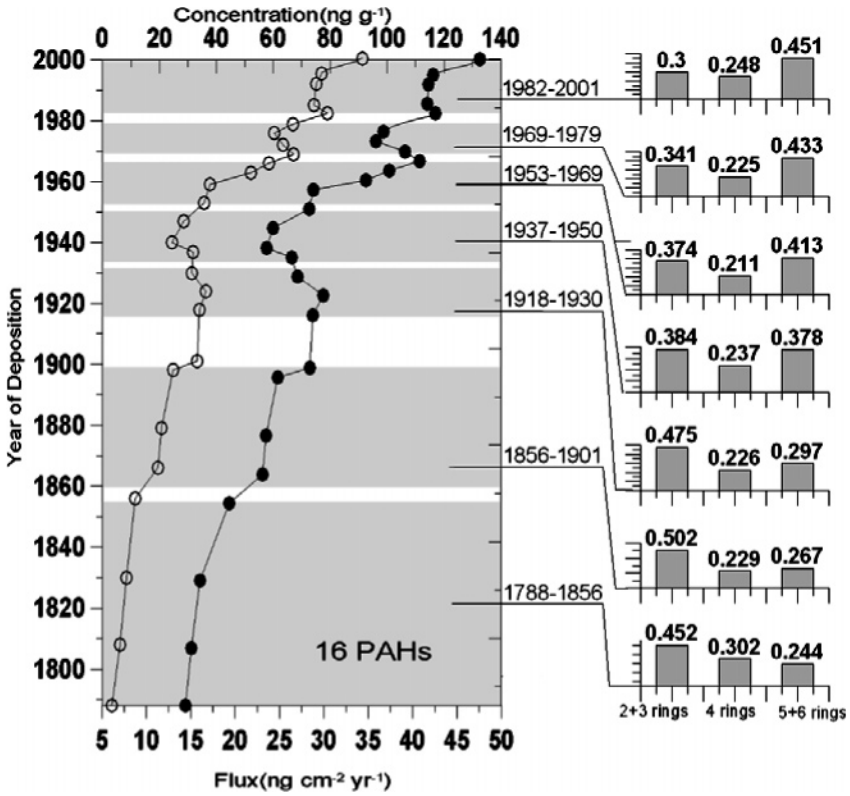

FIGURE 2. Concentration (dots) and depositional flux (circles) profiles of TPAHs and average relative distributions of 2 + 3, 4, and 5 + 6 rings USEPA priority PAHs at the different time stages in sediment core DM1.

downwind of the Chinese Mainland and the pathway for outflow continental pollutants to the northern Pacific in spring and winter, resulting in a large deposition of atmospheric particles on the ECS and YS (*22*, *23*). Atmospheric input of metals such as Cu, Pb, Co, etc. to the YS is higher than riverine input (*23*). Thus DM is the ideal place to extract sediment core for the reconstruction of historical record of airborne contaminants transported mainly from China.

Materials and Methods

Sample Collection. DM1 is located at 125°45′ E and 31°45′ N (Figure 1). Its water depth is 63 m. The sediment core was collected using a gravity corer in September 2003. The length of sediment core was 121 cm, and the diameter is 9 cm. The core was mainly clayey silt (Figure S1). The down-core variation of the grain size was small, indicating a stable dynamic sedimentary environment in the DM. The core was stored upright at 4 °C in the ship. In the laboratory, the core was cut into 1-cm samples along the length using a stainless steel cutter. The samples were packed in Al foil and stored at −20 °C until analysis.

Organic Analysis. The PAH analysis procedure followed that described by Mai et al. (*5*). Briefly, homogenized samples were freeze-dried and ground. About 10 g of the sample was spiked with a mixture of recovery standards of five deuterated PAHs (naphthalene-d_8, acenaphthene-d_{10}, phenanthrene-d_{10}, chrysene-d_{12}, and perylene-d_{12}). The samples were extracted with dichloromethane in a Soxhlet extractor for 72 h, with activated copper added to remove the sulfur in the samples. The extract was concentrated and fractionated using a silica−alumina (1:1) column. PAHs and polar components were eluted using 35 mL of hexane/dichloromethane (1:1) and 25 mL of methanol, respectively. The PAHs fraction was concentrated to 0.5 mL, and hexamethylbenzene was added as internal standard. The mixture was further reduced to 0.2 mL and subjected to GC-MSD analysis. A HP-5972 mass spectrometer interfaced to a HP-5890 II gas chromatography was used to analyze the samples. The GC was equipped with a HP-5 capillary column (25 m × 0.25 mm i.d., film thickness 0.25 μm), with He as carrier gas. The chromatographic conditions were as follows: injector temperature, 290 °C; detector temperature, 300 °C; temperature program: 80 °C (5 min), 80−290 °C at 4 °C min^{-1}, held at 290 °C for 30 min. The 21 PAHs quantified were as follows: naphthalene (NAP), acenaphthylene (AC), acenaphthene (ACE), fluorene (FLU), phenanthrene (PHE), methylphenanthrene (MP), dimethylphenanthrene (DMP), trimethylphenanthrene (TMP), quatermethylphenanthrene (QMP), anthracene (ANT), fluoranthene (FLUO), pyrene (PYR), benz[*a*]anthracene (BaA), chrysene (CHR), benzo[*b*]fluoranthene (BbF), benzo[*k*]fluoranthene (BkF), benzo[*a*]pyrene (BaP), indeno[1,2,3-*cd*]-pyrene (INP), dibenz[*a,h*]anthracene (DBA), perylene (PER), and benzo[*ghi*]perylene (BghiP). Procedural blanks, standard-spiked blanks, standard-spiked matrix, and parallel samples were analyzed for quality assurance and control. Recovery was 51.6 ± 12.2% for naphthalene-d_8, 62.8 ± 10.7% for acenaphthene-d_{10}, 94.9 ± 14.5% for phenanthrene-d_{10}, 64.7 ± 5.3% for chrysene-d_{12}, and 60 ± 10.6% for perylene-d_{12}. PAH concentrations were recovery corrected.

Dating of the Sediment Core. The dating of the sediment core followed the method described by Zhang et al. (*24*). Briefly, ^{210}Pb activities in the samples are determined by analyzing the α radioactivity of the decay product ^{210}Po by assuming they are in equilibrium. Po was extracted, purified, and self-plated onto silver disks at 75−80 °C in 0.5 M HCl, with Po used as yield monitor and tracer in quantification. Counting was conducted by computerized multichannel α spectrometry with gold-silicon surface barrier detectors. Supported ^{210}Po was obtained by indirectly determining the α activity of the supported parent ^{226}Ra, which was carried by coprecipitated $BaSO_4$. The average depositional rate is determined to be 0.31 cm yr^{-1} (Table S1 and Figure S2) which is in agreement with that reported by DeMaster et al. (*15*),

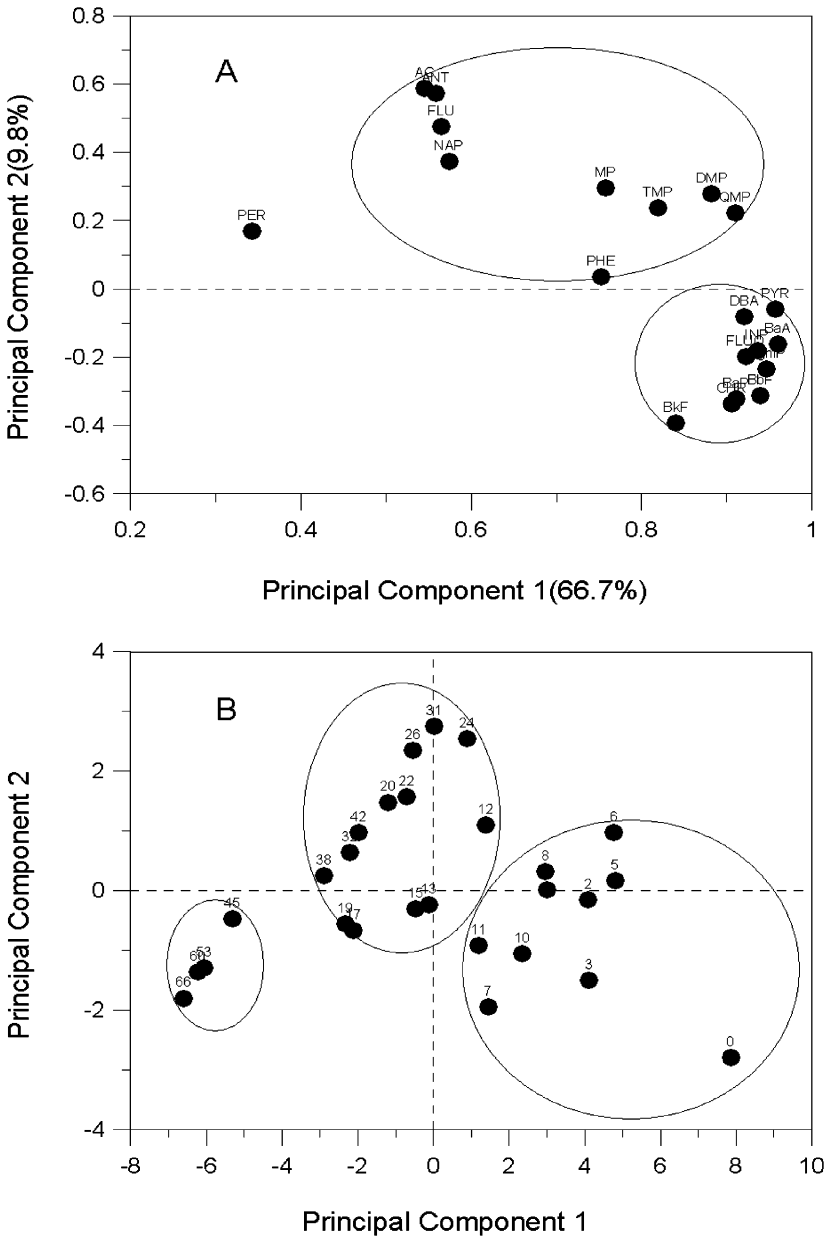

FIGURE 3. Principal components analysis for PAHs at DM1 sediment core samples: (A) loadings and (B) scores (0 means 0−1 cm layer, 10 for 10−11 cm layer, and so on in part B).

suggesting that this is the largest modern depositional rate in the DM.

Results and Discussion

Abundance and Flux of TPAH. Only the portion of the core from the top to 67 cm (~200 yr) was analyzed for PAHs. Concentrations and depositional fluxes are in Tables S2 and S3. USEPA proposed 16 priority PAHs as references for the evaluation of anthropogenic pollution in the environment (*10*). All these 16 PAHs were detected except for ACE and DBA in several layers of the core. TPAH (containing only the 16 USEPA priority PAHs) concentration and depositional flux profiles are shown in Figure 2. TPAH ranged from 27 to 132 ng g^{-1} (all weights are dry weight except otherwise specified). Depositional fluxes of TPAH were 6−34 ng cm^{-2} yr^{-1}. The down-core TPAH profiles of concentration and depositional flux tracked each other closely due to the stable dynamic environment in the DM.

The TPAH concentration profile closely follows the historical economic development of this region mainly for China. Prior to 1840, average low TPAH (27−32 ng g^{-1}) reflected the pollution level in an almost completely agricultural economy in China (*25*).

From 1856 to 1900, TPAH concentration gradually increased to the 42−69 ng g^{-1} level. This is the period after the Opium War (1840) when China was forced to open up for trading and started to industrialize under the "Westernization Movement" in the 1860s.

In the 37 years from 1901 to 1937, TPAH ranged from 69 to 78 ng g^{-1} and peaked in 1920s. The Great Depression in 1930s did not seem to slow down the development in China as in North America and Europe. From 1927 to 1936, China's industrial growth was maintained at 9.3%, and cities with populations in the millions such as Shanghai and Tianjing began to form (*25*). This period of prosperity in modern China is reflected accordingly by the PAHs in the core samples.

From 1937 to 1940, TPAH dropped from 69 to 57 ng g^{-1} (−17%), and this concentration was maintained until 1949. This showed the effect of WWII (1937−1945) and the Chinese Civil War (1946−1949). Many of the factories were moved

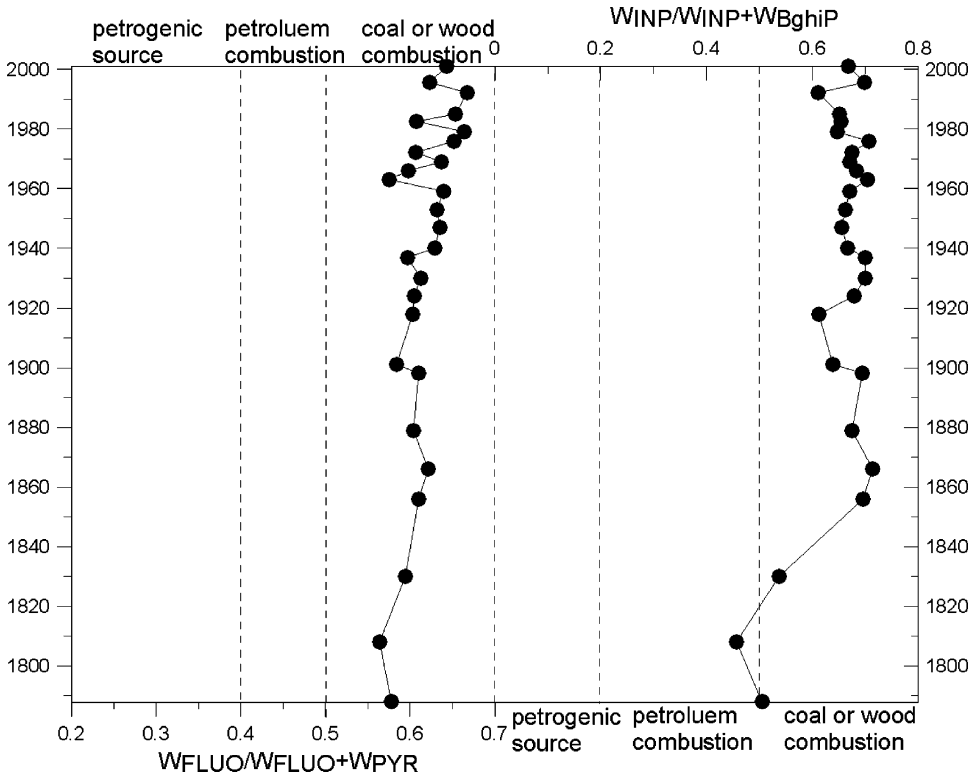

FIGURE 4. FLUO/(FLUO + PYR) and INP/(INP + BghiP) profiles for source identification. PAH source diagnostic ratios are from ref *3*.

from coastal areas to the southwest provinces to avoid attack and occupation by the Japanese during WWII, and those not moved sustained severe damages in the coastal areas of China (*25*, *26*). After WWII, this situation continued until 1949 due to the severe Chinese Civil War.

After the establishment of the People's Republic of China (PRC) in 1949, China entered a period of reconstruction and rapid economic development. From 1953 to 1958, it was 18%; 1958−1962 it was 3.8%; and 1963−1966 it was 13.3% (*27*). As a result, TPAH increased from 59 to 110 ng g^{-1} (+92%) from 1949 to 1969 in the DM1.

During the Cultural Revolution (CR) in China (1966−1976), many of the manufacturing plants either ceased to operate or greatly reduced production especially in the later period of this political movement; consequently, TPAH decreased from 110 to 96 ng g^{-1}. Similar trends were also observed in the Pearl River Delta by Liu et al. (*28*).

After CR, economic development recovered and with the initiation of the "Reform and Open" Policy in 1978, China entered the fastest industrialization (urbanization) period ever experienced, and it has been sustained until today. At the same time, the demand for energy from fossil fuels for power generation and transportation drastically increased (Figures S3 and S4) and compromised the environment. From 1982 to 2001, TPAH increased 35%, from 98 to 132 ng g^{-1}.

Lima et al. (*12*) reported the first peak of the high-resolution depositional fluxes of pyrogenic PAHs in the U.S. Eastern sediment core before the Great Depression. They subsided briefly before peaking again 1940 with the highest values in the 1950s. Another peak was observed starting in 1996. Similar trends in 1950−1970s were also observed by other researchers (*8*, *10*). The decline of these PAHs since 1950−1960s has been attributed to the switch from coal to oil and natural gas as energy sources (*8*, *10*, *12*). The increase of pyrogenic PAHs since 1996 may be due to the increased usage of diesel fuel by heavy-duty vehicles (*12*). The PAH depositional records extracted from European remote mountain lakes showed similarities to the U.S. trends (*13*). Because of the difference in energy structure, the vertical PAH distribution trends in China are therefore different from United States and Europe. These trends further indicate the difference in the economic development stages between these areas. China's energy still mainly relies on coal although the usage of petroleum has had a big increase since the 1980s (*27*).

Energy Structure Change in China, 1850−Present. In Figure 2, the 16 USEPA PAHs are grouped into 2 + 3 rings (NAP, AC, ACE, FLU, PHE, and ANT), 4 rings (FLUO, PYR, BaA, and CHR), and 5 + 6 rings (BbF, BkF, BaP, INP, DBA, and BghiP). Prior to 1900, 2 + 3 ring PAHs constituted an average of about one-half of the TPAH, while since 1920−1930s, this group of PAHs gradually decreased until it was only an average of 30% of TPAH in recent years (1982−2001) even 20% in 2001. In the past 200 years, the 5 + 6 ring group increased from an average of 24% (1788−1856) to the current value of 45% (1982−2001) even 53% in 2001, with a much faster increase in the second half of the 20th century (Figure S5). Low molecular weight (2 + 3 rings) PAHs are mostly contributions from low- and moderate-temperature combustion processes (biomass and coal burning in homes and small factories) and petrogenic sources (*4*, *5*), while high molecular weight (5 + 6 rings) PAHs are products of high-temperature combustion processes involving coal and petroleum such as large power plants and factories, vehicular emissions, and gas-fired cooking utensils (*5*, *29*, *30*). The change in energy structure from low- and moderate-temperature to high-temperature processes reflects the inevitable transformation from an agricultural economy to an industrial economy in China. This is especially evident after the initiation of the "Reform and Open" Policy in 1978.

Source Identification of PAHs. Ratios of PAHs with similar molecular weights have been used as indices for source apportionment (*2*−*5*, *31*). MP (total 4 isomers) /PHE can be used to differentiate petrogenic and pyrogenic PAHs. MP/PHE of pyrogenic PAHs is < 1, while it is 2−6 for the petrogenic PAHs (*5*, *32*). ANT/(ANT + PHE) and BaA/(BaA+CHR) ratios are often used together for this purpose. In general, when ANT/(ANT + PHE) < 0.1 and BaA/(BaA+CHR) < 0.2, a

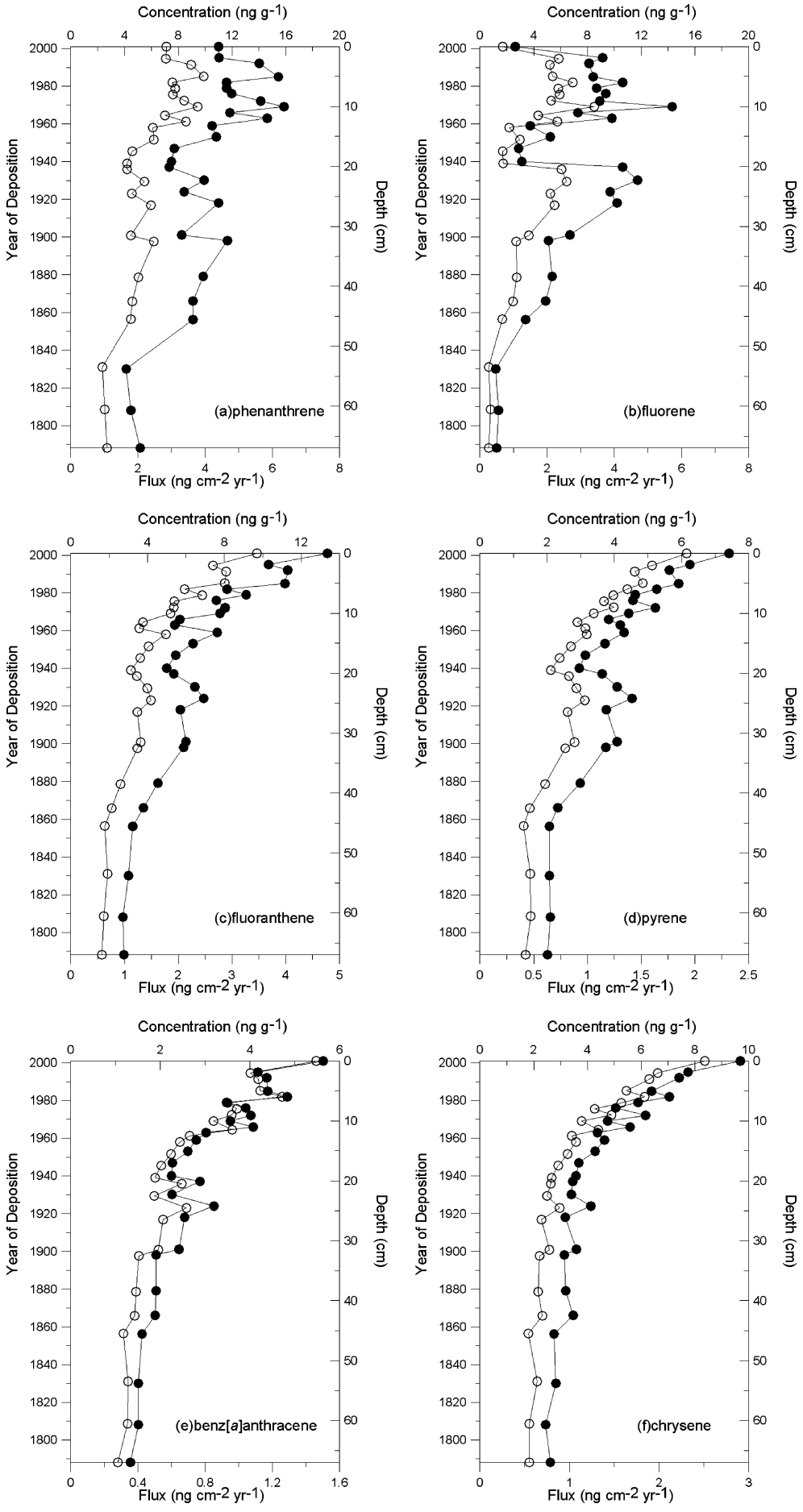
Concentration (ng g-1)
Year of Deposition
Depth (cm)
Flux (ng cm-2 yr-1)
(a)phenanthrene
(b)fluorene
(c)fluoranthene
(d)pyrene
(e)benz[a]anthracene
(f)chrysene

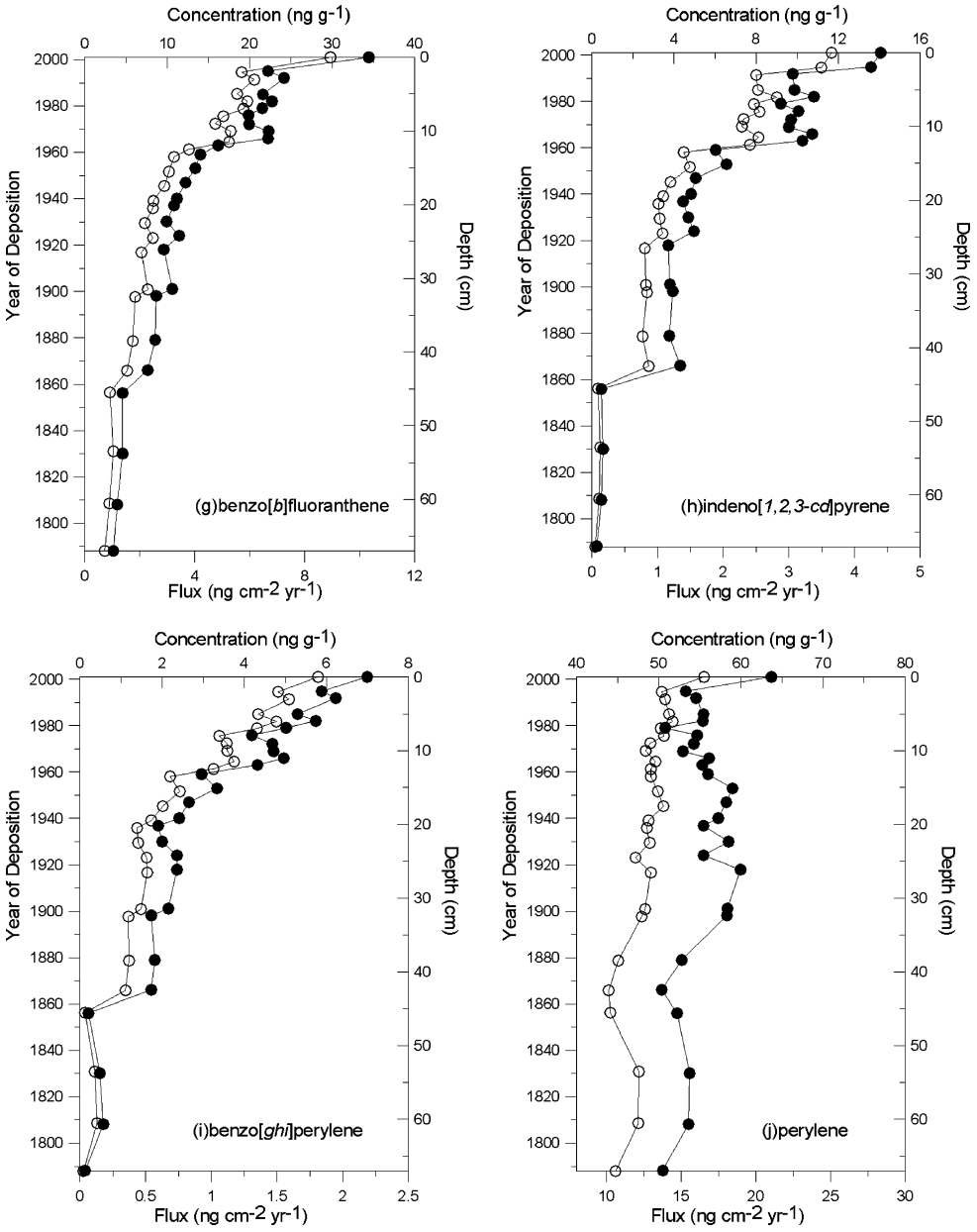

FIGURE 5. Concentration (dots) and depositional flux (circles) profiles of selected individual PAHs.

petrogenic source is suggested; for a pyrogenic source, ANT/(ANT + PHE) would be > 0.1 and BaA/(BaA+CHR) > 0.35 (*6*, *33*). MP/PHE was 0.4−1.0, ANT/(ANT + PHE) was 0.06−0.22, and BaA/(BaA+CHR) was 0.34−0.46, suggesting that a pyrogenic source was dominant in our samples.

FLUO/(FLUO+PYR) ratios < 0.4 are for a petrogenic source, between 0.4 and 0.5 for liquid fossil fuel (vehicle and crude oil) combustion, while ratios > 0.5 are characteristics of coal, grass, or wood combustion (*3*, *31*); INP/(INP+BghiP) ratios < 0.2 are possibly for a petrogenic source, between 0.2 and 0.5 for liquid fossil fuel (vehicle and crude oil) combustion, and ratios > 0.5 are for coal, grass, and wood combustion (*3*, *5*). Figure 3 indicates that the pyrogenic PAHs in the samples are mainly from the incomplete combustion of coal or biomass burning. In the past 20 years there has been a drastic increase in the consumption of petroleum products in China, and this is reflected in the depositional records in the Pearl River Delta sediment close to South China (*4*, *5*); however, this is not pronounced in the present study area for reasons to be stated below. (1) The main energy source in China is still coal. The energy consumption for 2000 is 69.0% coal, 22.3% oil, and 2.5% natural gas (*27*). (2) The sampling site is influenced by regions in North China that use extra coal for space heating in winter. The PAHs in the winter aerosols are 14 times higher than in the summer in the North China coastal city (*20*). Thus comparing to Southern China, coal is expected to contribute more to the sediments. (3) Biomass burning is still an important energy source in the villages in Northern China (*34*). All these make coal and biofuel the dominant origins of the PAHs in the core sample reasonable.

Source Apportionment Using Principle Component Analysis (PCA). Based on the loading of all measured PAHs (except ACE due to low concentration), PCA results in Figure 3A and Table S4 showed that there were three principal components (PC1, PC2, and PC3) accounting for 66.1%, 9.8%, and 6.3%, respectively, of the total variance. PC1 had a high positive loading of high molecular weight PAHs (FLUO, PYR, BaA, CHR, BbF, BkF, BaP, INP, DBA, and BghiP) attributable to high-temperature combustion sources. PC2 had a high positive loading of low molecular weight PAHs (NAP, AC, FLU, PHE, MP (4 isomers), and ANT) and could be considered to be contributions from petrogenic and low-temperature pyrogenic sources. PC3 was characterized by a high loading

of PER, indicating a different source and could originate from the diagenetic alteration of terrestrial organic matter. Based on sample scores, PCA results in Figure 3B and Table S5 showed that the core samples could be generally divided into three groups: the upper layer (0−12 cm, 1966−2001) characterized by the relatively high concentrations of 5 + 6 ring PAHs and the middle (12−43 cm) and bottom layers (45−67 cm) characterized by relatively high concentrations of 2 + 3 ring PAHs, indicating the change in the energy structure of China.

Concentration and Depositional Flux Variations of Selected PAHs. The more stable and abundant PAHs (PHE, FLU, FLUO, PYR, BaA, CHR, BbF, INP, BghiP, and PER) are important tracers for source identification, and their concentrations and depositional fluxes are shown in Figure 5.

PHE and FLU are mainly from low- and moderate-temperature combustion processes such as biomass burning and domestic coal burning (*4*, *5*, *29*, *30*), with a smaller contribution from petrogenic sources (*6*). The individual trends followed that of TPAH but became different after 1985 when the concentrations significantly decreased. This suggests that after 1985, there was a change in energy usage from low-temperature combustion to high-temperature combustion processes due to economic development needs.

The concentration and depositional flux profiles of FLUO and PYR are similar. They are tracers of coal and petroleum burning (*32*). The fluxes increased steadily and peaked in 1924. After 1949, except for a small drop during CR, concentrations and fluxes of FLUO and PRY gradually increased to the present level. BaA and CHR are dominant in the emissions of petroleum and the combustion process (*35*). The increase in BaA and CHR fluxes was small before 1949. The big increase came after 1949 and, even more pronounced, after 1980. These concentration and depositional flux profiles provide a close correspondence to the increasing energy demand for coal and petroleum in China.

The high molecular weight (HMW) BbF is a product of high-temperature combustion (*5*). It was the most abundant HMW PAH in the core sample. As with the other PAHs, BbF concentration increased rapidly after 1949. INP and BghiP have been used as tracers for vehicular exhaust (*29*, *36*). Just as the other pollutants, their concentrations, and fluxes increased rapidly in recent years, however, there is an anomaly, the concentrations increased during WWII. These PAHs, being indicators of vehicular emissions, suggest that the increase during WWII may be attributable to the large quantities of petroleum products used by the armed forces.

PER in sediment is thought to be from combustion processes (including fossil fuels and biomass) (*37*, *38*) and diagenesis of organic matter in anoxic sediments (*39*). The concentration variation of PER in the sample was totally different from the pyrogenic PAHs discussed above. Only at the top surface of the sample the concentration and depositional flux showed obvious increases, suggesting that PER was mainly natural, i.e., diagenesis of organic matter.

Acknowledgments

We wish to thank the crew of R/V of *Dong Fang Hong 2* of the Ocean University of China for extracting the core sample. Special thanks to the State Key Laboratory of Organic Geochemistry for organic analysis and ^{210}Pb dating. This work was supported by the Natural Science Foundation of China (NSFC) (Nos. 40276016 and 90211022) and the Ministry of Science and Technology of China ("973" Project No. 2005CB422304). The anonymous reviewers are sincerely appreciated for their critical reviews that greatly improved this paper.

Supporting Information Available

Tables of concentrations and fluxes for measured PAHs in each sediment sample, perdeuterated standard recoveries, figures of ^{210}Pb dating and measured data and annual GDP, and coal and oil consumption data from 1952 to 2000 in China, and PCA results. This material is available free of charge via the Internet at http://pubs.acs.org.

Literature Cited

(1) Hoffman, E. J.; Mills, G. L.; Latimer, J. S.; Quinn, J. G. Urban runoff as a source of polycyclic aromatic hydrocarbons to coastal waters. *Environ. Sci. Technol.* **1984**, *18*, 580−587.

(2) Yunker, M. B.; Snowdon, L. R.; Macdonald, R. W.; Smith, J. N.; Fowler, M. G.; Skibo, D. N.; Mclaughlin, F. A.; Danyushevskaya, A. I.; Petrova, V. I.; Ivanov, G. I. Polycylic aromatic hydrocarbon composition and potential sources for sediment samples from the Beaufort and Barents seas. *Environ. Sci. Technol.* **1996**, *30*, 1310−1320.

(3) Yunker, M. B.; Macdonald, R. W.; Vingarzan, R.; Mitchell, R. H.; Goyette, D.; Sylvestre, S. PAHs in the Fraser River Basin: a critical appraisal of PAH ratios as indicators of PAH source and composition. *Org. Geochem.* **2002**, *32*, 489−515.

(4) Mai, B. X.; Fu, J. M.; Zhang, G.; Lin, Z.; Min, Y. S.; Sheng, G. Y.; Wang, X. M. Polycyclic aromatic hydrocarbons in sediments from the Pearl River and estuary, China: spatial and temporal distribution and sources. *Appl. Geochem.* **2001**, *16*, 1429−1445.

(5) Mai, B. X.; Qi, S. H.; Zeng, E. Y.; Yang, Q. S.; Zhang, G.; Fu, J. M.; Sheng, G. Y.; Peng, P. A.; Wang, Z. S. Distribution of polycyclic aromatic hydrocarbons in the coastal region off Macao, China: assessment of input sources and transport pathways using compositional analysis. *Environ. Sci. Technol.* **2003**, *37*, 4855−4863.

(6) Baumard, P.; Budzinski, H.; Michon, Q.; Garrigues, T.; Burgeot, J. Origin and bioavailability of PAHs in the Mediterranean Sea from mussel and sediment records. *Estuarine, Coastal Shelf Sci.* **1998**, *47*, 77−90.

(7) Van Metre, P. C.; Mahler, B. J.; Furlong, E. T. Urban sprawl leaves its PAH signature. *Environ. Sci. Technol.* **2000**, *34*, 4064−4070.

(8) Simicik, M. F.; Eisenreich, S. J.; Golden, K. A.; Liu, S. P.; Lipiatou, E.; Swackhamer, D. L.; Long, D. T. Atmospheric loading of polycyclic aromatic hydrocarbons to lake Michigan as recorded in the sediments. *Environ. Sci. Technol.* **1996**, *30*, 3039−3046.

(9) Latimer, J. S.; Quinn, J. G. Historical trends and current inputs of hydrophobic organic compounds in an urban estuary: the sedimentary record. *Environ. Sci. Technol.* **1996**, *30*, 623−633.

(10) Pereira, W. E.; Hostettler, F. D.; Luoma, S. N.; Van Geen, A.; Fuller, C. C.; Anima, R. J. Sedimentary record of anthropogenic and biogenic polycyclic aromatic hydrocarbons in San Francisco Bay, California. *Mar. Chem.* **1999**, *64*, 99−113.

(11) Brenner, R. C.; Magar, V. S.; Ickes, J. A.; Abbott, J. E.; Stout, S. A.; Crecelius, E. A.; Bingler, L. S. Characterization and FATE of PAH-contaminated sediments at the Wyckoff/Eagle harbor superfund site. *Environ. Sci. Technol.* **2002**, *36*, 2605−2613.

(12) Lima, A. L.; Eglinton, T. I.; Reddy, C. M. High-resolution record of pyrogenic polycyclic aromatic hydrocarbon deposition during the 20th century. *Environ. Sci. Technol.* **2003**, *37*, 53−61.

(13) Fernandez, P.; Vilanova, R. M.; Martinez, C.; Appleby, P.; Grimalt, J. O. The historical record of atmospheric pyrolytic pollution over Europe registered in the remote mountain lakes. *Environ. Sci. Technol.* **2000**, *34*, 1906−1913.

(14) Hu, D. X. Upwelling and sedimentation dynamics I: The role of upwelling in sedimentation in the Yellow Sea and East China Sea. *Chin. J. Oceanol. Limnol.* **1984**, *2* (1), 12−19.

(15) DeMaster, D. J.; McKee, B. A.; Nittrouer, C. A.; Qian, J.; Cheng, G. Rates of sediment accumulation and particles reworking based on radiochemical measurements from shelf deposits in the East China Sea. *Cont. Shelf Res.* **1985**, *4*, 143−158.

(16) Milliman, J. D.; Qin, Y. S.; Park, Y. A. *Sediments and sedimentary processes in the Yellow and East China Seas. Sedimentary Facies in the Active Plate Margin*; Taira, A., Masuda, F., Eds.; Terra Scientific Publishing Company: Tokyo, 1989; pp 233−249.

(17) Milliman, J. D.; Beardsley, K. C.; Yang, Z. S.; Limeburner, R. Modern Huanghe derived muds on the outer shelf of the East China Sea: identification and potential mud-transport mechanisms. *Cont. Shelf Res.* **1985**, *4*, 37−45.

(18) Guo, Z. G.; Yang, Z. S.; Chen, Z. L.; Mao, D. Source of sedimentary organic matter in the mud areas of the East China Sea shelf. *Geochim.* **2001**, *30* (5), 416−424 (in Chinese).

(19) Simoneit, B. R. T.; Sheng, G. Y.; Chen, X.; Fu, J. M.; Zhang, J.; Xu, Y. Molecular marker study of extractable organic matter in aerosols from urban areas of China. *Atmos. Environ.* **1991**, *25A*, 2111−2129.
(20) Guo, Z. G.; Sheng, L. F.; Feng, J. L.; Fang, M. Seasonal variation of solvent extractable organic compounds in the aerosols in Qingdao, China. *Atmos. Environ.* **2003**, *37*, 1825−1834.
(21) Wilkening, K. E.; Barrie, L. A.; Engle, M. Trans-Pacific Air Pollution. *Science* **2000**, *290*, 65−67.
(22) Gao, Y.; Arimoto, R.; Duce, R. A.; Lee, D. S.; Zhang, M. Y. Input of atmospheric trace elements and mineral matter to the Yellow Sea during the spring of a low-dust year. *J. Geophys. Res.* **1992**, *97* (D4), 3767−3777.
(23) Zhang, J.; Huang, W. W.; Zhang, J.; Wang, Q. Transport of particulate heavy metals towards the esat China Seas: a preliminary study and comparison. *Mar. Chem.* **1992**, *40*, 161−178.
(24) Zhang, G.; Parker, A.; House, A.; Mai, B. X.; Li, X. D.; Kang, Y. H.; Wang, Z. S. Sedimentary records of DDT and HCH in the Pearl River Delta, South China. *Environ. Sci. Technol.* **2002**, *36*, 3671−3677.
(25) Zhang, K. Y. *Economic history of China*; Higher Education Press: Beijing, China, 2002; pp 178−326 (in Chinese).
(26) Zhu, G. D. The move of factories to Inland China and its effect on Inland industries. *J. Fudan University (Social Sci.)* **2001**, *4*, 43−50 (in Chinese).
(27) National Bureau of Statistics of China. *Statistics data on 55 years of new China*; China Statistics Press: Beijing, 2005 (in Chinese).
(28) Liu, G. Q.; Zhang, G.; Li, J.; Li, K. C.; Guo, L. L.; Liu, X.; Chi, J. S.; Peng, X. Z.; Qi, S. H. Over one hundred year sedimentary record of polycyclic aromatic hydrocarbons in the Pearl River Estuary, South China. *Environ. Sci.* **2005**, *26* (3), 141−145 (in Chinese).
(29) Harrison, R. M.; Smith, D. J. T.; Luhana, L. Source apportionment of atmospheric polycyclic aromatic hydrocarbons collected from an urban location in Birmingham, UK. *Environ. Sci. Technol.* **1996**, *30*, 825−832.
(30) Khalili, N. R.; Scheff, P. A.; Holsen, T. M. PAH source fingerprints for coke ovens, diesel and gasline engines, highway tunnels, and wood combustion emissions. *Atmos. Environ.* **1995**, *29*, 533−542.
(31) Oros, D. R.; Rose, J. R. Polycyclic aromatic hydrocarbons in San Francisco estuary sediments. *Mar. Chem.* **2004**, *86*, 169−184.
(32) Prahl, F. G.; Carpenter, R. Polycyclic aromatic hydrocarbon (PAH)-phase associations in Washington coastal sediment. *Geochim. Cosmochim. Acta* **1983**, *47*, 1013−1023.
(33) Hartmann, P. C.; Quinn, J. G.; Cairns, R. W.; King, J. W. The distribution and sources of polycyclic aromatic hydrocarbons in Narragansett Bay surface sediments. *Mar. Pollut. Bull.* **2004**, *48*, 351−358.
(34) Streets, D. G.; Gupta, S.; Waldhoff, S. T.; Wang, M. Q.; Bond, T. C.; Bo, Y. Y. Black carbon emissions in China. *Atmos. Environ.* **2001**, *35*, 4281−4296.
(35) Sicre, M. A.; Marty, J. C.; Saliot, A.; Aparicio, X.; Grimalt, J.; Albaiges, J. Aliphatic and aromatic hydrocarbons in different sized aerosols over the Mediterranean Sea: occurrence and origin. *Atmos. Environ.* **1987**, *21*, 2247−2259.
(36) Miguel, A. H.; Pereira, P. A. P. Benzo[k]fuoranthene, Benzo-[ghi]perylene, and Indeno[1, 2, 3-cd]pyrene : new tracers of automotive emissions in receptor modeling. *Aerosol Sci. Technol.* **1989**, *10*, 292−295.
(37) Blumer, M.; Blumer, W.; Reich, T. Polycyclic aromatic hydrocarbons in soils of a mountain valley: correlation with highway traffic and cancer incidence. *Environ. Sci. Technol.* **1977**, *11*, 1082−1084.
(38) Reddy, C. M.; Person, A.; Xu, L.; Mcnichol, A. P.; Benner, B. A.; Wise, S. A.; Klouda, G. A.; Currie, L. A.; Eglinton, T. I. Radiocarbon as a tool to apportion the sources of polycyclic aromatic hydrocarbon and black carbon in environmental samples. *Environ. Sci. Technol.* **2002**, *36*, 1774−1782.
(39) Venkatesan, M. I. Occurrence and possible sources of perylene in marine sediments - a review. *Mar. Chem.* **1988**, *25*, 1−27.

Received for review April 12, 2006. Revised manuscript received June 12, 2006. Accepted July 14, 2006.

ES060878B